

## Effective centrality and explosive synchronization in complex networks

A. Navas,<sup>1</sup> J. A. Villacorta-Atienza,<sup>2</sup> I. Leyva,<sup>1,3</sup> J. A. Almendral,<sup>1,3</sup> I. Sendiña-Nadal,<sup>1,3</sup> and S. Boccaletti<sup>4,5</sup>

<sup>1</sup>Center for Biomedical Technology, Univ. Politécnica de Madrid, 28223 Pozuelo de Alarcón, Madrid, Spain

<sup>2</sup>Department of Applied Mathematics, Facultad de Ciencias Matemáticas, Universidad Complutense, 28040 Madrid, Spain

<sup>3</sup>Complex Systems Group & GISC, Univ. Rey Juan Carlos, 28933 Móstoles, Madrid, Spain

<sup>4</sup>CNR-Institute of Complex Systems, Via Madonna del Piano, 10, 50019 Sesto Fiorentino, Florence, Italy

<sup>5</sup>Embassy of Italy in Israel, Trade Tower, 25 Hamered St., 68125 Tel Aviv, Israel

(Received 27 February 2015; revised manuscript received 3 July 2015; published 15 December 2015)

Synchronization of networked oscillators is known to depend fundamentally on the interplay between the dynamics of the graph's units and the microscopic arrangement of the network's structure. We here propose an effective network whose topological properties reflect the interplay between the topology and dynamics of the original network. On that basis, we are able to introduce the effective centrality, a measure that quantifies the role and importance of each network's node in the synchronization process. In particular, in the context of explosive synchronization, we use such a measure to assess the propensity of a graph to sustain an irreversible transition to synchronization. We furthermore discuss a strategy to induce the explosive behavior in a generic network, by acting only upon a fraction of its nodes.

DOI: [10.1103/PhysRevE.92.062820](https://doi.org/10.1103/PhysRevE.92.062820)

PACS number(s): 89.75.Hc, 05.45.Xt, 87.18.Sn

### I. INTRODUCTION

One of the most intriguing processes in complex networks' dynamics is synchronization: the spontaneous organization of the network's units into a collective dynamics. This phenomenon is known to be related to a delicate interplay between the topological attributes of the network and the main features of the dynamics of each graph's unit [1–3]. The conditions for synchronization in complex networks have been addressed by means of different approaches. For identical units, one of the most successful tools is the Master Stability Function [4], which rigorously shows how the spectral properties of the graph influence the stability of synchronization [1]. The general case of nonidentical units is far more complicated, and often needs a numerical approach, where the topology-dynamics relationship can only be investigated within specific scenarios [5–9]. However, several very recent works have obtained advances in the analysis of nonidentical network synchronization of phase oscillators ensembles, founding explicit bounds between the dynamics, the topology, and the coupling strength beyond which the system reaches phase synchronization [10,11], or how the basin stability depends on the structural-dynamics interplay [12].

Such a connection between structure and dynamics of a network is of particular importance in the case of the recently reported explosive synchronization (ES), an irreversible and discontinuous transition to the graph's synchronous state. Originally, ES was described in all-to-all coupled ensembles of Kuramoto oscillators [13] for a specific distribution of natural frequencies [14]. Later on, various kinds of degree-frequency correlations were found to be able to induce ES in networks of periodic and chaotic oscillators [15–18], or neural networks [19]. In addition, other microscopic mechanisms were proposed, based on diverse coupling strategies [20–22], or by introducing adaptive dynamics in a fraction of the network's units [23].

In this work, we propose the use of an effective topological network whose structure explicitly reflects the interplay between the topology and dynamics of the original system. On that basis, we introduce the *effective centrality* as a measure to

quantify the role of each node in the synchronization process. Using this measure, we reconsider the mechanisms underlying ES and revisit the main scenarios where such a behavior was previously reported. Finally, we formulate a criterion to induce explosive transitions by acting only on a fraction of the network's nodes.

### II. MODEL

We start by considering a network of  $N$  phase oscillators, whose instantaneous phases evolve in time according to the Kuramoto model [13]:

$$\dot{\theta}_i = \omega_i + \frac{\sigma}{N} \sum_{j=1}^N A_{ij} \sin(\theta_j - \theta_i), \quad i = 1, \dots, N, \quad (1)$$

where  $\theta_i$  is the phase of the  $i$ th oscillator,  $\omega_i$  its natural frequency [chosen from a generic, known, distribution  $g(\omega)$ ], and  $\sigma$  the coupling strength. The topology of the network is encoded in the adjacency matrix  $\mathbf{A}$  ( $A_{ij} = 1$  if node  $i$  is linked to node  $j$ , and  $A_{ij} = 0$  otherwise). The degree of a node is  $k_i = \sum_j A_{ij}$ . The level of synchronization is measured by the order parameter  $r = \frac{1}{N} \langle |\sum_{i=1}^N e^{i\theta_i}| \rangle_T$ , where  $|\cdot|$  and  $\langle \cdot \rangle_T$  denote module and time average, respectively. Throughout this work, the network size is fixed to  $N = 1000$  and the natural frequencies  $\omega_i$  are randomly drawn from a uniform distribution in the interval  $[-0.5, 0.5]$ , unless otherwise specified.

As the coupling strength  $\sigma$  gradually increases, system (1) experiences a transition from an incoherent ( $r \simeq 0$ ) to a frequency-synchronized, phase-locking state ( $r \simeq 1$ ), a process often referred to as path to synchrony (PTS) [24]. In heterogeneous networks, the PTS is mainly dominated by the most connected nodes (or hubs), which actually act as synchronization seeds, and progressively recruit the other network's nodes. At variance, in homogeneous networks, the PTS is characterized by the emergence of coherent clusters growing around multiple synchronization seeds. Along the PTS, the first nodes that locally synchronize generally correspond to pairs of connected oscillators whose natural frequencies are closer,

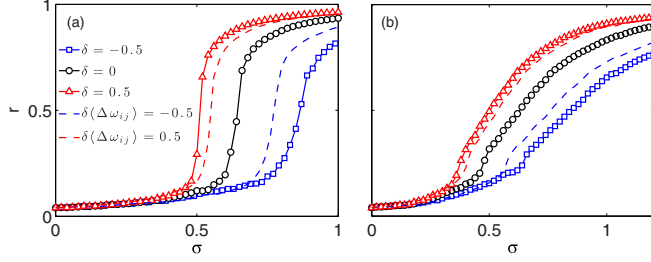


FIG. 1. (Color online) Synchronization transition curves (black circles) compared with the modified adjacency matrix  $A_{ij}(1 + \delta\Delta\omega_{ij})$  in (a) ER,  $\langle k \rangle = 30$  and (b) SF  $\langle k \rangle = 12$  networks for positive and negative  $\delta$  values. Red triangles ( $\delta > 0$ ) and blue squares ( $\delta < 0$ ) show how a local perturbation enhances/frustrates the synchronization more efficiently than a global perturbation over all links [dashed lines, where  $\delta\Delta\omega_{ij} \rightarrow \delta\langle\Delta\omega\rangle$ , being  $\langle\Delta\omega\rangle$  the average over nonzero values of the detuning matrix].

whereas the globally synchronized state emerges around those with natural frequencies close to the synchronization frequency  $\Omega_s$ . While traditionally attention has been focused on the natural dynamics of each node, recent works [21,22] have shown the importance of frequency detuning in the process of synchronization, motivating a different approach, where the links prevail over the nodes themselves. Hence, we propose the frequency detuning  $\Delta\omega_{ij} \equiv |\omega_i - \omega_j|$  between each pair of nodes as the relevant dynamical feature for the determination of the PTS. To formalize our idea, let us introduce a change of variables  $r_j e^{i\Psi_j} = \frac{1}{N} \sum_{k \in \Gamma_j} e^{i\theta_k}$ , where  $r_i(t)$  is a local order parameter and  $\Gamma_j$  is the set of neighbors of the node  $j$ . Substituting into Eq. (1) we obtain

$$\dot{\theta}_i = \omega_i + \sigma r_i \sin(\Psi_i - \theta_i). \quad (2)$$

It naturally follows that the velocity difference is  $\dot{\Phi}_{ij} = \dot{\theta}_i - \dot{\theta}_j = \omega_i - \omega_j + \sigma [r_i \sin(\Psi_i - \theta_i) - r_j \sin(\Psi_j - \theta_j)]$ . As frequency synchronization implies  $\dot{\Phi}_{ij} = 0$ , the set of links through which synchronization may take place must fulfill

$$\Delta\omega_{ij} \leq \sigma(r_i + r_j), \quad (3)$$

which in fact relates the local phase locking to the frequency detuning associated to the links, being those pairs of nodes with large detuning, which are harder to synchronize. To further show the role of frequency detuning, we investigate how a modification of the adjacency matrix by a certain function of the detuning affects the PTS, i.e.,  $\mathbf{A} \rightarrow \mathbf{A}f(\Delta\omega)$ . Considering a first-order approximation, it results in  $A_{ij} \rightarrow A_{ij}(1 + \delta\Delta\omega_{ij})$  for  $f(0) = 1$  and  $f'(0) = \delta$ . Figure 1 reports the synchronization transition curves for [Fig. 1(a)] Erdős-Reyni (ER) with a mean degree  $\langle k \rangle = 30$  [25] and [Fig. 1(b)] scale-free (SF) with  $\langle k \rangle = 12$  networks generated with the Barabasi-Albert algorithm [26]. It can be seen an enhancement (frustration) of the synchronization transition as  $\delta$  is increased (decreased). Hence, positive (negative) values of  $\delta$  potentiate (weaken) the strength of the couplings according to their  $\Delta\omega_{ij}$ . Notice that such a local perturbation of the adjacency matrix is more effective in promoting or delaying the PTS than a global perturbation of the same mean equally acting on all links as shown by the corresponding dashed lines in Fig. 1.

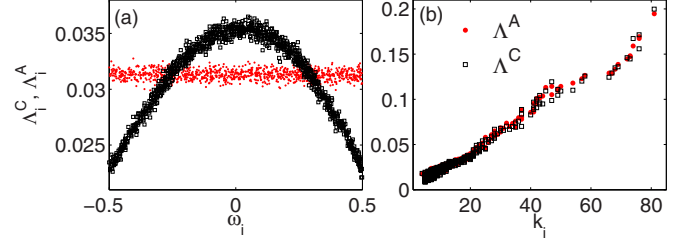


FIG. 2. (Color online) Comparison between synchronization centrality  $\Lambda_i^C$  (black squares) and topological centrality  $\Lambda_i^A$  (red dots). (a) ER networks,  $\langle k \rangle = 50$ ,  $\Lambda_i^C$ , and  $\Lambda_i^A$  are reported vs the nodes' natural frequencies  $\omega_i$ ; (b) SF networks,  $\langle k \rangle = 12$ ,  $\Lambda_i^C$ , and  $\Lambda_i^A$  are plotted vs the node degrees  $k_i$ . All data refer to ensemble averages over 100 different network realizations.

### III. EFFECTIVE CENTRALITY

Since we are concerned about extracting the dynamical backbone of the network composed by the seeds of synchronization and according to the above results, we introduce the following effective adjacency matrix in order to amplify their role:

$$C_{ij} \equiv A_{ij} \left( 1 - \frac{\Delta\omega_{ij}}{\Delta\omega_{\max}} \right), \quad (4)$$

where we have chosen  $f'(0) = -1/\Delta\omega_{\max}$ , being  $\Delta\omega_{\max}$  the maximum possible detuning present in the system in order to guarantee  $C_{ij} \geq 0$ . Within this specific choice of  $f'(\Delta\omega)$ ,  $C_{ij}$  results in an effective topological network that exhibits the structure of the original one but enhancing those more synchronizable pairs of nodes (i.e., those with small detuning) according to Eq. (3).

Now, in order to quantify the role of each node in the synchronization process, we extract the most important nodes in the effective network defined by  $\mathbf{C}$ , i.e., we calculate the standard eigenvector centrality measure [1,27–29] of  $\mathbf{C}$ , obtaining the effective centrality vector  $\Lambda^C$ . The  $i$ th component  $\Lambda_i^C \geq 0$  provides a measure of the importance of the node  $i$  in the effective network and quantifies its potential to behave as a seed of synchronization.

As a simple test for further clarifying the meaning of  $\Lambda_i^C$ , Fig. 2 shows the comparison between  $\Lambda^C$  and its topological counterpart  $\Lambda^A$ , the eigenvector centrality extracted from the original adjacency matrix  $\mathbf{A}$ . For Erdős-Rényi (ER) networks [25], the distribution of the components of the vector  $\Lambda^C$  as a function of the corresponding node's natural frequencies shows the existence of many seeds of synchronization with natural frequencies close to  $\Omega_s = 0$  [see the black squares of Fig. 2(a)]. This allows the characterization of the connection between the microscale (detuning of the links) and the macroscale (emergence of global synchronization) of the system in a much better way than  $\Lambda^A$ , whose components [red dots in Fig. 2(a)] are instead uniformly distributed. For heterogeneous scale-free (SF) networks [26], the synchronization seeds are the hubs and therefore  $\Lambda^C$  and  $\Lambda^A$  provide essentially the same information, as it can be seen in Fig. 2(b).

The previous result shows that the effective network allows us to highlight the importance of each node in the

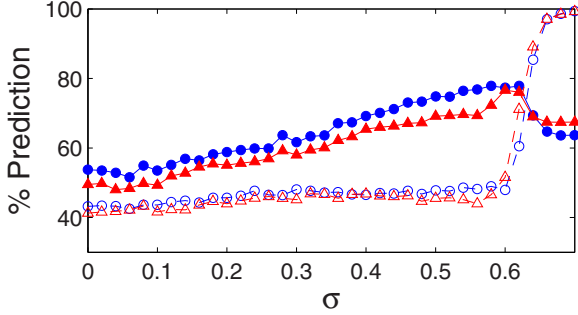


FIG. 3. (Color online) Average percentage of coincidence between the third of the nodes with the highest (red triangles) and lowest (blue circles) dynamical  $\Lambda_i^S$  and effective  $\Lambda_i^C$  centralities (solid symbols) and the corresponding percentage between dynamical  $\Lambda_i^S$  and topological  $\Lambda_i^A$  centralities (empty symbols). Calculations are performed on ER networks with  $\langle k \rangle = 50$ , and refer to 10 realizations of the network's topology and frequency distribution (see text for details).

PTS; we proceed with confronting our approach with a dynamical exploration of the system for the case of ER networks. Precisely, we calculate a local synchronization matrix  $\mathbf{S} = \{S_{ij}\} = A_{ij} |\langle e^{i\Delta\theta_{ij}} \rangle_t|$  [24] where  $\Delta\theta_{ij} = \theta_i - \theta_j$  and  $\sigma \in [0, 0.7]$ . The eigenvector centrality of  $\mathbf{S}$ , denoted by  $\Lambda^S$ , provides the actual synchronization centrality of each node in the synchronization process.

Mathematically, the Perron-Frobenius theorem states that if  $\mathbf{M}$  is an irreducible matrix, the effective centrality  $\Delta^M$  is well defined, i.e., exists and is unique. A  $N \times N$  matrix  $\mathbf{M}$  is irreducible if and only if its associated graph  $G_M$  is strongly connected, where  $G_M$  has  $N$  vertices and node  $i$  is connected to  $j$  when  $M_{ij} > 0$  [30]. Since both  $\mathbf{C}$  and  $\mathbf{S}$  are symmetric matrices, strongly connected means just that  $G_C$  and  $G_S$  are connected graphs. This fact is always verified in our simulations, therefore  $\mathbf{C}$  and  $\mathbf{S}$  matrices are irreducible. Notice that both  $\mathbf{C}$  and  $\mathbf{S}$  have essentially the connectivity of  $\mathbf{A}$ , since whenever  $A_{ij} = 1$  then  $C_{ij} > 0$  (except for one link that never contributes to disconnect  $G_C$ ), and  $S_{ij} > 0$ , since  $|\langle e^{i\Delta\theta_{ij}} \rangle_t| > 0$ .

In Fig. 3 we sort the nodes according to the increasing value of the corresponding centrality and we report the percentage of coincidence between the third of the nodes with the highest (lowest) synchronization  $\Lambda_i^S$  and effective  $\Lambda_i^C$  centralities (solid symbols), and the corresponding percentage of coincidence between the third of the nodes with the highest (lowest) synchronization  $\Lambda_i^S$  and topological  $\Lambda_i^A$  centralities (empty symbols). It can be seen that the ranking based on  $\Lambda_i^C$  is able to predict up to 80% of the nodes with the highest (lowest) dynamical centrality, while the topological centrality only detects at most 50%. According to  $\Lambda_i^C$  the maximum of predictability is reached around the synchronization threshold and decreases rapidly due to the homogenization of the synchronization matrix  $\mathbf{S}$  for overcritical couplings, while the predictability according to  $\Lambda_i^A$  is approximately constant until it increases to 100% when  $S_{ij} = 1$  ( $\mathbf{S} = \mathbf{A}$ ), that is, in the trivial completely synchronous state.

#### IV. EFFECTIVE CENTRALITY IN EXPLOSIVE SYNCHRONIZATION

As effective centrality reveals itself as a suitable measure to study the PTS, we move on to elucidating how this quantity helps us also to understand the microscopical mechanisms underlying explosive synchronization (ES). As it has been remarked in the introduction, ES can be induced when topology and dynamics are related in several specific ways [14–18, 20–23, 31]. Almost all these methods are based on a manipulation of the adjacency matrix and/or the links weights, such that in Eq. (1)  $A_{ij}$  is replaced by a certain matrix  $\Omega_{ij}$  which usually correlates the structural and dynamical features of the network.

To show how the different procedures impact the effective centrality vector, we compare the  $\Lambda^C$  associated with the non explosive case and the corresponding  $\Lambda^{\tilde{C}}$  when the explosive method is applied, that is,  $\tilde{C}_{ij} = \Omega_{ij} (1 - \frac{\Delta\omega_j}{\Delta\omega_{\max}})$ . Results for some of the different methods are condensed in Fig. 4 for ER (left panels) and SF (right panels) networks. In each panel,  $\Lambda_i^{\tilde{C}}$  (red dots) are plotted together with  $\Lambda_i^C$  (cyan dots) to show how the explosive method actually modifies the effective centrality vector and, therefore, the dynamical role of each node. Nodes are sorted in ascending order of  $\Lambda_i^C$ . In all the cases where the structural and dynamical correlations introduced through  $\Omega_{ij}$  successfully lead to ES [Figs. 4(a)–4(d), 4(f)], there is an increase (decrease) of  $\Lambda_i^{\tilde{C}}$  of those nodes whose  $\Lambda_i^C$  was low (high), that is, the weighting method produces a flattening of  $\Lambda_i^{\tilde{C}}$ . In this way, the potential ability of the nodes to behave as seeds of local synchronization is frustrated until a certain coupling strength is reached. Only once the coupling strength is large enough, the rest of the network fulfills the condition (3), and therefore a sudden transition to synchronization takes place.

Figures 4(a)–4(b) correspond to the method described in Ref. [21], where ES is achieved choosing  $\Omega_{ij} = A_{ij} |\omega_i - \omega_j|$  for ER networks (a) and  $\Omega_{ij} = A_{ij} |\omega_i - \omega_j| l_{ij} / \sum_j l_{ij}$  for SF networks (b), being  $l_{ij}$  the edge betweenness [1]. Figures 4(c)–4(d) show, instead, the case  $\Omega_{ij} = A_{ij} |\omega_i| / k_i$  proposed in Ref. [31] for uniform frequency distributions centered in zero. It is easy to see that the above increase-decrease compensation is fulfilled for both ER [Fig. 4(c)] and SF [Fig. 4(d)] networks. As expected, in SF networks the modification affects mainly the hubs, thwarting their dynamical influence as seeds, and frustrating the PTS. Finally, Fig. 4(f) reports the case of ES induced in SF networks by imposing a frequency-degree correlation  $\omega_i = k_i$  [15]. Here the effect is focused on the hubs (see the inset), whose effective centrality is now strongly decreased, while the imposed correlation does not produce a substantial difference between  $\Lambda^{\tilde{C}}$  and  $\Lambda^C$  for the rest of the nodes. There are, however, cases when, even if the structure and dynamics are correlated, ES does not occur. For instance, Fig. 4(e) reports the same case presented in Fig. 4(c) but for positive definite frequencies. And indeed, for this frequency distribution, it is seen that the weighting method fails to flatten sufficiently  $\Lambda^C$  (the red horseshoe cloud), with the consequence that ES fails to emerge as well.

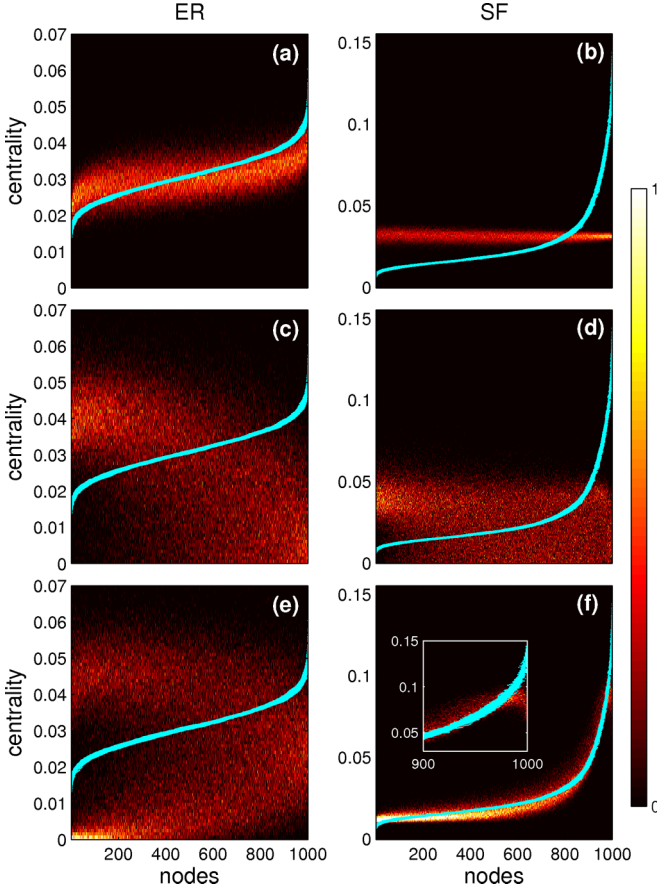


FIG. 4. (Color online) Effective centrality of explosive networks ( $\Lambda_i^C$ , red clouds) versus that of non-explosive networks ( $\Lambda_i^C$ , cyan clouds) for ER (left panels) and SF (right panels) topologies (see text for definitions). (a) and (b) account for the weighted method of Ref. [21] with a uniform natural frequency distribution in  $[-0.5, 0.5]$ . (c) and (d) correspond to the weighted method of Ref. [31] with the same uniform frequency distribution (see text for the methods' description). (e) is the same as in (d) but natural frequencies are here chosen from the positive values of a Gaussian distribution, in a way that ES is no longer induced. Finally, (f) corresponds to a SF network where the degree-frequency correlation method from Ref. [15] is applied and the same uniform frequency distribution as for (a)–(d) is used. The inset in (f) is a zoom centered on the highest-degree nodes. All data refer to averages over 100 realizations.

## V. TARGETED EXPLOSIVE SYNCHRONIZATION

A possible application of our effective centrality is the engineering of a strategy to produce ES in a generic network by only acting upon a small fraction of its nodes, according to a given ranking defining their role as synchronization seeds. We here test four possible rankings: (i) the effective ranking based on  $\Lambda_i^C$ ; (ii) the distance ranking, which sorts the nodes according to the distance  $\Delta\Lambda_i^C = |\Lambda_i^C - \Lambda_i^{\tilde{C}}|$ ; (iii) the topological ranking, based on  $\Lambda_i^A$ ; and, finally, (iv) a random ranking, which is used for comparison. These specific rankings are actually suggested by the characteristic PTS occurring in both ER and SF networks, where the increase-decrease condition and the dominant role of hubs constitutes, respectively, the essential feature (see Fig. 4).

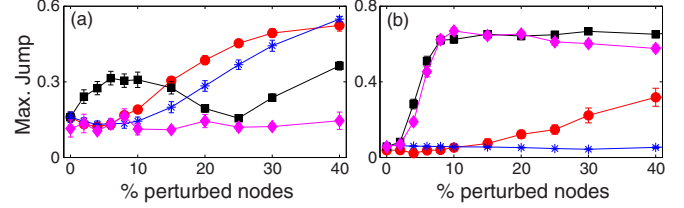


FIG. 5. (Color online) Maximum jump size in the synchronization curve  $\sigma(r)$  vs fraction of perturbed nodes chosen along several rankings: effective (back squares), distance (red dots), topology (magenta diamonds), and random (blue asterisks). (a) ER networks ( $k = 30$ , weighting method from Ref. [21]). (b) SF networks ( $k = 6$  imposing  $\omega_i = k_i$  for the selected nodes as in Ref. [15]). In all cases, data refer to averages over 50 realizations.

Figure 5 reports the jump in the discontinuous synchronization transition curve for all the rankings as a function of the % of perturbed nodes affected by the weighting methods of Refs. [15, 21]. The discontinuity jump is calculated as  $\max[r(\sigma + \delta\sigma) - r(\sigma)]$ , the maximal difference found in the order parameter between two consecutive  $\sigma$  values. For homogeneous ER networks [Fig. 5(a)], we choose a given % of ranked nodes and weight their links as  $\Omega_{ij} = A_{ij}|\omega_i - \omega_j|/\bar{\Omega}_{ij}$ , where  $\bar{\Omega}_{ij}$  is the mean of the nonzero elements of  $\Omega$  [32]. The rest of the nodes remain with the original adjacency. The effective ranking (black squares) indicates that a significant explosive effect is obtained in the network already for just 6% of the nodes but decreases afterwards, whereas the distance ranking (red circles) requires up to 15% to get an equivalent jump, inducing a complete explosive transition for percentages above 30%. In comparison, using a random ranking it is necessary to manipulate at least the 40% of the nodes, while the topological ranking is not able to induce ES in this interval.

For SF networks [Fig. 5(b)], we use instead the degree-frequency correlation as in Ref. [15], setting  $\omega_i = k_i$  for the corresponding first percentage of nodes along the ranking. In this case, both the effective (black squares) and topological (magenta diamonds) rankings clearly outperforms the distance ranking (red circles) by only affecting the 10% of the nodes. In comparison, the random ranking is not able to induce ES even above the 40%.

The differences between ER and SF cases are due to the different ways the seeds spread in the network. In the ER case, the effective ranking performs better for small percentages since it focuses on the seeds of synchronization. As soon as this percentage increases, the nodes with the lowest  $\Lambda^C$  are not longer captured, and the increase-decrease condition is not fulfilled. As there are multiple randomly distributed seeds, the distance ranking is only slightly better than the random one, as both satisfy the increase-decrease condition once the percentage is large enough. In the SF case the topology is determinant as the seeds are just a few hubs, allowing to induce ES acting upon a very small fraction of the nodes of the network, whereas the random targeting is definitely not the suitable choice.

In conclusion, we have introduced an effective network whose topological properties quantitatively characterize the

PTS of networked oscillators, contributing to a deeper knowledge of the synchronization process. Even if the recent developments [10,11] have advanced in this direction, our approach allows us to reveal the individual role of the nodes in the synchronization path, and in particular the inner mechanisms beneath ES, which are shown to be rooted in a frustration of the PTS. Finally, it also allows us to control such behavior locally, since we have the means to identify and isolate those seeds involved in the emergence of synchronization.

## ACKNOWLEDGMENTS

The authors acknowledge the computational resources and assistance provided by CRESCO, the supercomputational center of ENEA in Portici, Italy. Work partly supported by the Spanish Ministerio de Economía y Competitividad under Projects FIS2012-38949-C03-01 and FIS2013-41057-P, and by the INCE Foundation under the Project INCE2014-011. I.L., J.A., and I.S.N. acknowledge support from GARECOM, Group of Research Excellence URJC-Banco de Santander.

- 
- [1] S. Boccaletti, V. Latora, Y. Moreno, M. Chavez, and D. U. Hwang, *Phys. Rep.* **424**, 175 (2006).
- [2] S. N. Dorogovtsev, A. V. Goltsev, and J. F. F. Mendes, *Rev. Mod. Phys.* **80**, 1275 (2008).
- [3] A. Arenas, A. Díaz-Guilera, J. Kurths, Y. Moreno, and C. S. Zhou, *Phys. Rep.* **469**, 93 (2008).
- [4] L. M. Pecora and T. L. Carroll, *Phys. Rev. Lett.* **80**, 2109 (1998).
- [5] Y. Moreno and A. F. Pacheco, *Europhys. Lett.* **68**, 603 (2004).
- [6] E. Oh, K. Rho, H. Hong, and B. Kahng, *Phys. Rev. E* **72**, 047101 (2005).
- [7] J. G. Restrepo, E. Ott, and B. R. Hunt, *Chaos* **16**, 015107 (2006).
- [8] A. Arenas, A. Diaz-Guilera, and C. J. Perez-Vicente, *Phys. Rev. Lett.* **96**, 114102 (2006).
- [9] C. Zhou and J. Kurths, *Chaos* **16**, 015104 (2006).
- [10] F. Dörfler, M. Chertkov, and F. Bullo, *Proc. Natl. Acad. Sci. USA* **110**, 2005 (2013).
- [11] P. S. Skardal, D. Taylor, and J. Sun, *Phys. Rev. Lett.* **113**, 144101 (2014).
- [12] P. J. Menck, J. Heitzig, J. Kurthsand, and H. J. Schellnhuber, *Nature Commun.* **5**, 3969 (2014).
- [13] Y. Kuramoto, *Chemical Oscillations, Waves and Turbulence* (Springer, Berlin, 1984).
- [14] D. Pazó, *Phys. Rev. E* **72**, 046211 (2005).
- [15] J. Gómez-Gardeñes, S. Gómez, A. Arenas, and Y. Moreno, *Phys. Rev. Lett.* **106**, 128701 (2011).
- [16] I. Leyva, R. Sevilla-Escoboza, J. M. Buldú, I. Sendiña-Nadal, J. Gómez-Gardeñes, A. Arenas, Y. Moreno, S. Gómez, R. Jaimes-Reátegui, and S. Boccaletti, *Phys. Rev. Lett.* **108**, 168702 (2012).
- [17] P. Li, K. Zhang, X. Xu, J. Zhang, and M. Small, *Phys. Rev. E* **87**, 042803 (2013).
- [18] P. S. Skardal and A. Arenas, *Phys. Rev. E* **89**, 062811 (2014).
- [19] H. Chen, G. He, F. Huang, C. Shen, and Z. Hou, *Chaos* **23**, 033124 (2013).
- [20] I. Leyva, A. Navas, I. Sendiña-Nadal, J. A. Almendral, J. M. Buldú, M. Zanin, D. Papo, and S. Boccaletti, *Sci. Rep.* **3**, 1281 (2013).
- [21] I. Leyva, I. Sendiña-Nadal, J. A. Almendral, A. Navas, S. Olmi, and S. Boccaletti, *Phys. Rev. E* **88**, 042808 (2013).
- [22] X. Zhang, Y. Zou, S. Boccaletti, and Zonghua Liu, *Sci. Rep.* **4**, 5200 (2014).
- [23] X. Zhang, S. Boccaletti, S. Guan, and Z. Liu, *Phys. Rev. Lett.* **114**, 038701 (2015).
- [24] J. Gómez-Gardeñes and Y. Moreno, *Phys. Rev. E* **73**, 056124 (2006).
- [25] P. Erdős and A. Rényi, *Publicationes Mathematicae* **6**, 290 (1959).
- [26] A. L. Barabási and R. Albert, *Science* **286**, 509 (1999).
- [27] E. Fuchs, A. Ayali, E. Ben-Jacob, and S. Boccaletti, *Phys. Biol.* **6**, 036018 (2009).
- [28] Chun-Hsien Li and Suh-Yuh Yang, *Phys. Lett. A* **378**, 1239 (2014).
- [29] Z. He, X. Wang, G.-Y. Zhang, and M. Zhan, *Phys. Rev. E* **90**, 012909 (2014).
- [30] C. D. Meyer, *Matrix Analysis and Applied Linear Algebra* (SIAM, Philadelphia, 2001).
- [31] X. Zhang, X. Hu, J. Kurths, and Z. Liu, *Phys. Rev. E* **88**, 010802(R) (2013).
- [32] This normalization guarantees the presence of both reinforced and weakened links in the network, with the weighted adjacency matrix having values equal, larger, and lower than one.